Title: Simultaneous removal of Cr(VI) and 4-chlorophenol through photocatalysis by a novel anatase/titanate nanosheet composite: Synergetic promotion effect and autosynchronous doping

Author: Wen Liu Weiling Sun Alistair G.L. Borthwick Ting Wang Fan Li Yidong Guan

PII: S0304-3894(16)30557-X
DOI: http://dx.doi.org/doi:10.1016/j.jhazmat.2016.06.002
Reference: HAZMAT 17791

To appear in: *Journal of Hazardous Materials*

Received date: 16-3-2016
Revised date: 1-6-2016
Accepted date: 2-6-2016

Please cite this article as: Wen Liu, Weiling Sun, Alistair G.L.Borthwick, Ting Wang, Fan Li, Yidong Guan, Simultaneous removal of Cr(VI) and 4-chlorophenol through photocatalysis by a novel anatase/titanate nanosheet composite: Synergetic promotion effect and autosynchronous doping, Journal of Hazardous Materials http://dx.doi.org/10.1016/j.jhazmat.2016.06.002

Simultaneous removal of Cr(VI) and 4-chlorophenol through photocatalysis by a novel anatase/titanate nanosheet composite: Synergetic promotion effect and autosynchronous doping

Wen Liu [a, c,*], Weiling Sun[b], Alistair G.L. Borthwick[d], Ting Wang[b], Fan Li[c], Yidong Guan[a, c,*]

[a] *Jiangsu Key Laboratory of Atmospheric Environment Monitoring and Pollution Control, School of Environmental Science and Engineering, Nanjing University of Information Science and Technology, Nanjing 210044, China*

[b] *The Key Laboratory of Water and Sediment Sciences, Ministry of Education, Department of Environmental Engineering, Peking University, Beijing 100871, China*

[c] *Environmental Engineering Program, Department of Civil Engineering, Auburn University, Auburn, AL 36849, USA*

[d] *6FKRRO RI (QJLQHHULQJ 7KH 8QLYHUVLW\ RI (GLQEXUJK 7KH LQQ [illegible] Edinburgh EH9 3JL, UK*

* Corresponding authors

W. Liu, Tel: +1-334-444-7129; Fax: +1-334-844-6290;

E-mail: wzl0025@auburn.edu

Y. Guan, Phone: +86-25-5873-1090; Fax: +86-25-5873-1090;

E-mail: yidongguan@nuist.edu.cn

Graphical abstract

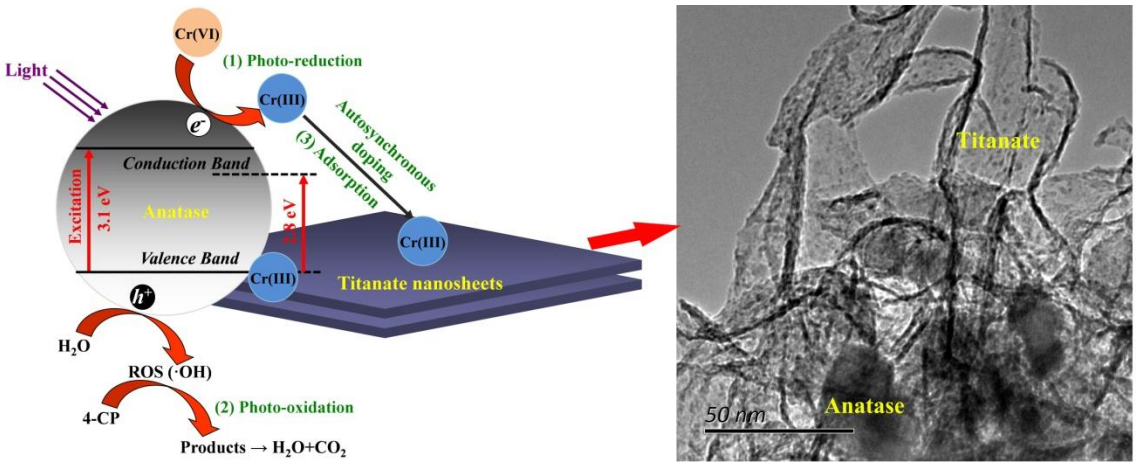

Highlights

- TNS composed of anatase and titanate synthesized via a facile one-step method
- Cr(VI) and 4-CP can be simultaneously removed by TNS through photocatalysis
- Photocatalytic efficiencies of Cr(VI) and 4-CP greatly enhanced when coexisting
- Synergetic promotion effect occurs due to separation of electron-hole pairs
- Autosynchronous doping after Cr(III) adsorption leads to narrowed energy gap

Abstract

Clean-up of wastewaters with coexisting heavy metals and organic contaminants is a huge issue worldwide. In this study, a novel anatase/titanate nanosheet composite material (labeled as TNS) synthesized through a one-step hydrothermal reaction was demonstrated to achieve the goal of simultaneous removal of Cr(VI) and 4-cholophenol (4-CP) from water. TEM and XRD analyses indicated the TNS was a nano-composite of anatase and titanate, with anatase acting as the primary

photocatalysis center and titanate as the main adsorption site. Enhanced photocatalytic removal of co-existent Cr(VI) and 4-CP was observed in binary systems, with apparent rate constants (k_1) for photocatalytic reactions of Cr(VI) and 4-CP about 3.1 and 2.6 times of that for single systems. In addition, over 99% of Cr(VI) and 4-CP was removed within 120 min through photocatalysis by TNS at pH 7 in the binary system. Mechanisms for enhanced photocatalytic efficiency in the binary system are identified as: (1) a synergetic effect on the photo-reduction of Cr(VI) and photo-oxidation of 4-CP due to efficient separation of electron-hole pairs, and (2) autosynchronous doping because of reduced Cr(III) adsorption onto TNS. Furthermore, TNS could be efficiently reused after a simple acid-base treatment.

Keywords: Titanate nanosheet; Synergetic promotion; Autosynchronous doping; Photocatalysis; Combined pollution

1. Introduction

Industrial wastewaters offer substantial threats to the environment and human health. Such wastewaters usually contain a complicated mixture of constituents, often involving co-existence of multiple contaminants, such as heavy metals and organic pollutants [1-3], requiring expensive, difficult technological treatment often targeted at the removal of certain pollutants. For example, Cr(VI) and chlorinated phenols (CPs) are found to coexist in tannery wastewaters [4, 5]. Cr(VI) is a commonly encountered heavy metal with high toxicity, resulting from its carcinogenicity and teratogenicity [6]. CPs are emerging contaminants and persistent organic pollutants

(POPs) that are widespread in wastewaters originating from certain industrial processes, such as tanning, and manufacturing of preservatives, pesticides and antifouling agents [7, 8]. Although many techniques, including adsorption, membrane, bio-process, direct chemical oxidation, and advanced oxidation processes (AOPs, like Fenton reaction), are used to resolve pollution problems involving Cr(VI) or/and CPs [9-16], these treatment processes are relatively inefficient, high-cost and complicated to operate. Moreover, methods which completely remove Cr(VI) through reduction and degradation of CPs are undoubtedly better than those based purely on adsorption or phase separation. Therefore, development of highly efficient, inexpensive technologies for the treatment of combined polluted wastewaters is urgently required in the environmental remediation area.

Photocatalysis using titanium related nanomaterials (including TiO_2 and titanate) seems a good choice for solving the very difficult problem of reduction of Cr(VI) and complete degradation of CPs in industrial wastewaters [17, 18]. TiO_2 is the most common photocatalyst used for degradation of organic compounds including CPs [19-21]. In recent years, the particularly effective ion-exchange property of titanate nanomaterials (especially titanate nanotubes, TNTs) has led to their widespread use as metal-cation adsorbents (e.g. Pb(II), Cd(II), Cr(III), radionuclides, etc.) [22-26]. However, pure titanate possesses two main defects: (1) low adsorption capacity for metal anions (like Cr(VI) and As(V)) and organics [27-29], and (2) weak photocatalytic activity because of the immediate recombination of photo-generated electron-hole pairs [18, 30-32]. Therefore, combination of TiO_2 and titanate would

appear to be a sensible method for simultaneous removal of both heavy metals and organics through initial photocatalysis and subsequent adsorption. In this way, Cr(VI) can be photo-reduced to Cr(III) by TiO_2 and then adsorbed by titanate, and organic compound (e.g. CPs) can be directly photo-degraded in the meanwhile. Although previous studies have paid attention to the photocatalytic reduction of Cr(VI) by TiO_2 or combination of TiO_2 and TNTs [17, 18], and to the photocatalytic degradation of CPs by single TiO_2 [19, 33], there is little information available on the simultaneous removal of Cr (including both Cr(VI) and Cr(III)) and CPs through photocatalysis and adsorption. An understanding still needs to be built up of the mechanism underlying this complex system.

Given the above context, we propose a facile one-step method to synthesize a composite anatase/titanate nanosheet (labeled as TNS), composed of TiO_2 and titanate, with good adsorptive and photocatalytic properties. The prepared TNS was used to remove coexisting Cr(VI) and 4-CP simultaneously. The main objectives of this study are: (1) preparation of a titanate-based material for effective simultaneous removal of both Cr(VI) and 4-CP; (2) to achieve complete removal of Cr(VI) and Cr(III) using the fore-going titanate-based material; (3) to elucidate mechanisms for photocatalytic removal of isolated and co-existing Cr(VI) and 4-CP; and (4) to test reusability of the synthesized material.

2. Experimental

2.1 Chemicals

All chemicals used in this study were of analytical grade or better, and used without further purification. Nano-scale TiO_2 (anatase, 99.7%, mean size of 25 nm), used as a precursor to synthesize TNS, was purchased from Sigma-Aldrich (St. Louis, MO, USA). NaOH (purity > 98.0%) and absolute ethanol (also used to synthesize TNS) were obtained from Acros Organics (Fair Lawn, NJ, USA). Analytical $K_2Cr_2O_7$, $CrCl_3 \cdot 6H_2O$ and 4-CP were purchased from Acros Organics (Fair Lawn, NJ, USA). Deionized (DI) water (0LOOLSRUH R 0LP) was used to prepare all the solutions.

2.2 Preparation and characterization of TNS

TNS was synthesized through a short-cut hydrothermal method [34]. Specifically, 0.8 g of TiO_2 powder was added into 80 mL of 8 mol/L NaOH solution and stirred for 12 h. The mixture was then transferred into a Teflon reactor and heated at 130 °C for 3 h. Afterwards, the suspension was washed with DI water until the supernatant was neutral. Finally, TNS was dispersed with ethanol and obtained after drying at 80 °C for 4 h. Pure titanate (TNTs) was also synthesized through the same hydrothermal process but heated for 6 h [34].

Morphology of the TNS was measured using Tecnai F30 FEG transmission electron microscopy (TEM, FEI, USA) operating at 300 kV, and energy dispersive spectra (EDS) were collected meanwhile. The crystal phase structure of the sample was identified by means of a Dmax/2400 X-ray diffractometer (XRD, Rigaku, Japan) with Cu .. radiation source (= 1.5418 Å) at a scan rate (2) of 4°/min. Specific surface area of TNS was determined using an ASAP 2010 adsorption apparatus

(Micromeritics, USA) through nitrogen adsorption-desorption isotherms at -196 °C according to Brunauer-Emmett-Teller (BET) theory. Elemental composition and oxidation state were obtained by an AXIS-Ultra X-ray photoelectron spectroscopy (XPS, Kratos, England) using Al .. X-ray at 15 kV and 15 mA. The standard C 1s peak (Binding energy, E_b = 284.80 eV) was used to eliminate the static charge effects. During measurement, the nitrogen adsorption volume was set to a relative pressure (P/P_0) of 0.99. Zeta potentials of the materials under various pH were detected using a Nano-ZS90 Zetasizer (Malvern Instruments, UK), in order to determine the point of zero charge (pH_{PZC}). UV-vis diffuse reflectance spectra (DRS) of the materials were obtained by a UV-2400 spectrophotometer (Shimadzu, Japan) using the Kubelka-Munk function.

2.3 Adsorption of Cr and 4-CP by TNS

Adsorption of Cr(VI), Cr(III), and 4-CP by TNS was tested at different solution pH. With 5 mg/L of Cr or 4-CP mixed with 0.025 g TNS to form a total solution of 50 mL, the pH of the mixture was adjusted from 2 to 9 using dilute HCl or NaOH solution. After the sample was shaken (200 rpm, 25±2 qC) for 4 h and filtered through PSROWHWUDIOXRURHWKHQH37)(PHPEUDQHWKH4-CP concentration in the supernatant was determined. Adsorption of Cr(VI), Cr(III) and 4-CP by anatase and pure titanate was also tested at different pH under the same conditions, respectively. All the adsorption experiments were conducted in dark.

Total Cr concentration was measured using an inductively coupled plasma-mass (ICP-MS, X Series II, Thermo Fisher Scientific, USA). Cr(VI) concentration was

determined through a dinitrodiphenyl carbazide spectrophotometric method at 540 nm by a UV-vis spectrophotometer (UV1800, Shimadzu, Japan). Cr(III) concentration was calculated as the difference between total Cr and Cr(VI) concentrations. 4-CP concentration was measured using high performance liquid chromatography (HPLC, Agilent 1200 Series, USA) equipped with a C18 column (SB-AQ, 5 P 4.6 mm × 250 mm) and a diode array detector (DAD). A mixture of methanol (HPLC grade, BDH, USA) and ultrapure water (v/v of 60:40) provided the mobile phase. Samples were injected into the HPLC instrument at a flow rate of 1 mL/min and analyzed at an UV absorbance wavelength of 280 nm. Adsorption capacity (q_e) and removal efficiency (R) of Cr or 4-CP are calculated from:

$$q_e \quad \frac{(C_0 \quad C_e)V}{m} \tag{1}$$

$$R \quad \frac{(C_0 \quad C_e)}{C_0} \quad 100\% \tag{2}$$

where q_e (mg/g) is the adsorption capacity of Cr or 4-CP on TNS at equilibrium; C_0 and C_e (mg/L) are the initial and equilibrium concentrations of Cr or 4-CP; V (L) is the total volume of the solution, and m (g) is the mass of added TNS.

2.4 Photocatalysis of Cr(VI) and 4-CP by TNS

Photocatalytic experiments were carried out in a cuboid quartz reactor (total volume of 300 mL, 5×5×12 cm) as shown in Fig. S1. A high-pressure mercury lamp (150 W, 365 nm) was used as the UV light source, which was placed beside the reactor with cooling air supplied to maintain the reaction temperature of 25±2 qC. The UV light density in the reactor center was measured as 2.5 mW/cm^2. The photocatalytic tests were carried out for the following scenarios: (1) photocatalysis of

isolated Cr(VI) and 4-CP, the reaction initiated by mixing 5 mg/L of Cr(VI) or 4-CP (200 mL in total volume) with 0.5 g/L TNS; and (2) photocatalysis of coexisting Cr(VI) and 4-CP, the reaction initiated using a fixed Cr(VI) concentration of 5 mg/L, and coexisting 4-CP concentrations of 2.5, 5 and 10 mg/L. All the foregoing photocatalytic tests were repeated for pH 5, 7 and 9. Blank photocatalytic tests were also carried out without materials under UV light. Photocatalytic experiments of Cr(VI) and 4-CP by pure anatase and titanate were also carried out respectively for comparison. TNS with Cr(III) (TNS-Cr(III)) after co-removal of Cr(VI) and 4-CP were collected for EDS, XPS and UV-vis DRS analysis.

Langmuir-Hinshelwood (L-H) model is introduced to describe the photocatalysis process, whereby the rate of change of time-dependent concentration C_t (mg/L) is expressed as [35-37] :

$$\frac{dC_t}{dt} \quad r \quad k_r \frac{K_L C_t}{1 \quad K_L C_t} \tag{3}$$

in which r (mg/(LÂmin)) is the photocatalytic reaction rate, k_r (mg/(LÂmin)) is the photocatalytic reaction rate constant, K_L (L/mg) is the Langmuir constant for adsorption, and t is time. For $K_L C_t << 1$, $t = 0$ and $C_t = C_0$, Equation (3) simplifies to the first-order kinetic model:

$$\ln(C_0 / C_t) \quad k_1 t \tag{4}$$

where k_1 (min^{-1}) is the first-order apparent rate constant.

The degradation intermediates of 4-CP were also determined using a gas chromatograph-mass spectrometer (GC-MS, Agilent 7890A GC coupled with 5975C Series mass spectrometry) and the detailed method is described in **Supplementary**

data. In addition, the amount of hydroxyl radicals ($^{\bullet}OH$) formed in the photocatalysis reaction was detected by a photoluminescence (PL) technique as shown in **Supplementary data**.

2.5 Material reuse

After photocatalysis of coexisting Cr(VI) and 4-CP, both at concentration 5 mg/L and pH 7, TNS was filtered though a 0.22 PTFE membrane and air-dried for reuse. More specifically, 0.2 g of TNS was immersed in 0.5 mol/L HNO_3 (500 mL) for 8 h to desorb Cr(III), and the resulting TNS material immersed in 0.5 mol/L NaOH (500 mL) for 8 h in order for regeneration to occur. The resulting TNS was then reused for photocatalysis of coexisting Cr(VI) and 4-CP at pH 5, with the proposed photocatalysis-desorption-regeneration process lasting 5 cycles.

3. Results and discussion

3.1 Morphology and crystal structure of TNS

Fig. S2 and Fig. 1 show the morphologies of nano-TiO_2 and TNS obtained using TEM. The procurer nano-TiO_2 particle is a kind of nano-sphere, with mean diameter of 25 nm (Fig. S2). After hydrothermal treatment, these TiO_2 nanoparticles transformed into nanosheets, which are more like ribbons (Fig. 1a). High resolution TEM (HRTEM) further indicates that each of the ribbons has uniform interlayer distance of 0.70 nm, in accordance with the crystalline plane of titanate (020) (Fig. 1b) [38]. Anatase crystalline titanium dioxide (101) also can be observed in TNS (Fig. 1c) [39], suggesting the synthesized TNS is a composite material containing both titanate and anatase.

[Fig. 1]

Fig. 2 presents the XRD patterns obtained for nano-TiO_2 and TNS. For TiO_2, the peaks all belong to crystalline anatase (JCPDS 21-1272) [40, 41]. After synthesis of TNS, the peaks at 25.3q, 37.9q, 53.9q and 54.9q ascribed to anatase still remain, notably the A(101) peak. However, new peaks at 9.6q, 28.4q, 48.1q and 62.7q attributed to crystal diffraction of titanate are also present [22, 26, 42]. The peak at 9.6q (020) represents the interlayer distance of titanate, which is 0.70 nm for the TNS prepared in this study (Fig. 1b) [22, 26, 38]. Moreover, the resulting titanate nanosheet is a kind of sodium tri-titanate with chemical formula given by $Na_xH_{2-x}Ti_3O_7$ (in which x = 0í 0.75, depending on the remaining sodium content), and composed of layered corrugated ribbons formed through edge-sharing of triple [TiO_6] octahedrons forming a skeletal structure and H^+/Na^+ located in interlayers [22, 26].

[Fig. 2]

The prepared TNS exhibits large specific surface area of 147.9 m^2/g and total single pore volume of 0.47 cm^3/g (Fig. S3). The N_2 adsorption-desorption isotherms of TNS are consistent with type IV isotherms with H3 hysteresis loops, according to BDDT classification (Fig. S3a), indicating the presence of mesopores (2±50 nm) in the material [43]. Due to the low point of zero charge (pH_{PZC} = 3.2) (Fig. S4), TNS can easily capture metal cations (Cr(III) in this study), followed by ion-exchange with the interlayered H^+/Na^+ (primary Na^+) [14, 22].

For the formation of TNS, The Ti±O±Ti bonds between the [TiO_6] octahedron will be broken to planer fragments under NaOH treatment during the hydrothermal

process, and then the fragments reassemble and link together, resulting in the formation of hydroxyl bridges between two fragments and triple end-sharing [TiO_6] octahedrons, thus forming tianate nanosheets [34, 38, 44]. By control the hydrothermal time (3 h in this study), partial reorganization of anatase crystal lattices to tri-tianate results in the formation of anatase-covered titanate composite (TNS).

3.2 Adsorption of Cr(VI), Cr(III) and 4-CP by TNS

Fig. 3 displays the adsorption capacities of Cr(VI), Cr(III) and 4-CP by TNS over a pH range from 2 to 9. The variations in Cr(VI) and Cr(III) adsorption capacities with increasing pH are entirely different. The adsorption capacity of Cr(VI) decreases almost monotonically over the pH range considered, falling from 1.9 to 0.8 mg/g as pH increases from 2 to 3, and then reaching ~0 mg/g by pH • . In addition, the Cr(VI)-adsorption capacity was invariable quite small (<2 mg/g) regardless of pH due to the low pH_{PZC} of TNS (3.2). Here, Cr(VI) existed as oxyanions (mainly $HCrO_4^-$ and CrO_4^{2-}) at pH 2í 9 (Fig. S5a), and so the less positively charged (pH ”3) or negatively charged (pH •4) TNS can hardly capture these Cr(VI) anions. Conversely, the Cr(III)-adsorption capacity increased with increasing pH, saturating at a pH of about 5. At pH values of 2 and 3, positively charged TNS adsorbed fewer Cr(III) cations (Cr^{3+} and $Cr(OH)^{2+}$) (Fig. S5b). However, TNS underwent was a charge transformation for TNS from pH 3 to 4 (Fig. S4), leading to a substantial increase in Cr(III) adsorption capacity from 2.1 to 7.6 mg/g. For further increase in pH, the more negative charge located on TNS resulted in a larger adsorption capacity, reaching 9.7 mg/g at pH 5 in conjunction with a high removal efficiency of 97.1%. Precipitation of Cr(III)

($Cr(OH)_3$ formation) occurred for pH • 6, associated with enlarged Cr(III) adsorption capacity. The overall adsorption behaviors of Cr(VI) and Cr(III) by TNS as functions of pH are similar to results obtained using TNTs [18, 27], due to the similar basic composition of sodium tri-titanate. Similar results were found for adsorption of Cr(VI) by both pure anatase and titanate (Fig. S6). However, adsorption behaviors of Cr(III) differed a lot, as the adsorption capacity of titanate was much larger than that of anatase, resulting from the abundant í ONa/H groups locating on the titanate, which can efficiently capture Cr(III) cations through ion-exchange [22, 45]. The adsorption capacity of Cr(III) was ranked as titanate >TNS >>anatase.

[Fig . 3]

The adsorption capacity of 4-CP was relatively low (<0.4 mg/g) regardless of change in pH. Considering the inorganic structure of TNS (sodium titanate) and 4-CP with a pK_a value of 9.41 [46], the material is almost unable to capture molecular 4-CP over the pH range (2í 9) of the tests. Similarly, the inorganic pure anatase and tianate could hardly adsorb 4-CP (Fig. S6). Therefore, adsorption on its own is not viable as a treatment process for removal of Cr(VI) and 4-CP; instead, auxiliary photocatalysis is necessary.

3.3 Photocatalysis of Cr(VI) and 4-CP by TNS in the single system

Solution pH values of 5, 7 and 9 were selected to represent acidic, neutral and alkaline conditions to study their effects on photocatalysis. Fig. 4 shows removal of total Cr and Cr(VI), as well as the formation of Cr(III) over time. For Cr(III), the non-dimensional concentration C_t/C_0 is obtained as the ratio of concentration of Cr(III)

formed in the aqueous solution to the initial total Cr concentration. It can be seen that the total Cr and Cr(VI) in the aqueous solution gradually decreased as irradiation time increased. Almost no Cr(III) accumulated in solution except during the first hour at pH 5, leading to nearly overlapping concentration-time curves for total Cr and Cr(VI). Therefore, the reduced Cr(III) could be immediately and continuously adsorbed by TNS, mainly the titanate phase with high adsorptive property. Moreover, no Cr(III) could be detected at 210 min, indicating all the reduced Cr(III) was adsorbed onto TNS finally, which is consistent with the adsorption results (Fig. 3). Formation and removal of Cr(III) simultaneously occurred within the solution; i.e. Cr(III) formed through photocatalytic reduction of Cr(VI) was immediately adsorbed by TNS. Precipitation of Cr(III) at higher pH resulted in its more rapid removal, and so no Cr(III) could be detected even at 10 min for pH 7 and 9.

Photocatalytic reduction of Cr(VI) by TNS occurred more quickly at lower pH, as reflected in the higher apparent rate constant (k_1) (Table 1). When pH increased from 5 to 9, the k_1 value decreased from 0.0240 to 0.0087 min^{-1}, indicating lower photocatalytic activity of TNS for Cr(VI) reduction under alkaline conditions. Moreover, no Cr(III) remained in solution at 210 min under any of the conditions considered, and so the final Cr (total) and Cr(VI) removal efficiency was identical, with values of 99.6%, 97.2% and 84.8% at pH 5, 7 and 9, respectively. Considering the high adsorption capacity for Cr(III) (Fig. S6), titanate played the dominant role in removal of reduced Cr(III). The present results concerning the effect of pH are consistent with those of previous studies, which reported acidic conditions facilitate

photo-reduction of Cr(VI) [18, 47, 48]. Here, the H^+-included reactions proceed as:

$$H_2CrO_4 + 6H^+ + 3e^- = Cr^{3+} + 4H_2O \quad (5)$$

or

$$HCrO_4^- + 7H^+ + 3e^- = Cr^{3+} + 4H_2O \quad (6)$$

It appears that existence of abundant H^+ should be beneficial to reduction of Cr(VI) oxyanions. However, presence of OH^- ions would inhibit Cr(VI) reduction because:

$$CrO_4^{2-} + 4H_2O + 3e^- = Cr(OH)_3 + 5OH^- \quad (7)$$

[Fig . 4]

Unlike Cr(VI), selection of higher pH enhanced 4-CP photo-degradation (Fig. 5). The k_1 value for 4-CP photocatalytic degradation increased from 0.0221 min^{-1} for pH 5 to 0.0399 min^{-1} for pH 9 (Table 1). It is worth noting that although photocatalytic activity of TNS for 4-CP photo-degradation varied with pH, the removal rates were invariably above 99% by 210 min, indicating the extremely high efficiency of TNS for 4-CP removal. OH^- anions promote formation of hydroxyl radicals (‡OH), which are primary reactive oxygen species (ROS) for oxidation of organic compounds [49], and the mechanism will be further discussed in detail later in Section 3.5.

[Fig . 5]

It is noteworthy that almost no Cr(VI) and 4-CP could be photocatalytically removed by pure titanate, as the photocatalytic curves are almost the same to blank results (only photolysis without materials) (Fig. S7). Therefore, the photocatalytic activity of pure titanate was very weak due to easy recombination of excited

electron-hole pairs. However, anatase showed high removal efficiencies for Cr(VI) (97.8 %) and 4-CP (99.8 %) even after 180 mins of photocatalysis at pH 7 (Fig. S7), and high k_1 values of 0.0247 min^{-1} and 0.0354 min^{-1}, respectively. The photocatalytic activity of the concerned materials followed the sequence of anatase >TNS >>titanate. Given the different adsorption capacities and photocatalytic activities of different materials, it is indicated that TNS is an intermediate material from anatase to titanate, which has the advantages of the both anatase and titanate.

3.4 Photocatalysis of Cr(VI) and 4-CP by TNS in the binary systems

The single system tests in Section 3.3 have shown that increasing pH promoted photo-reduction of Cr(VI) but inhibited photo-degradation of 4-CP. Consequently, the solution pH was set to 7 to achieve both high removal efficiencies of Cr(VI) and 4-CP in binary systems. Fig. 6a plots the removal of coexisting Cr(VI) and 4-CP at same initial concentration (5 mg/L) in the photocatalytic process, and the corresponding results for single systems are also plotted for comparison. Removal of Cr(VI) was greatly promoted by coexistence of 4-CP, with the associated k_1 value (0.0502 min^{-1}) being about 3.1 times that for Cr(VI) photo-reduction without 4-CP (0.0164 min^{-1}). The total Cr and Cr(VI) removal efficiencies attained values as high as 99.7 % at 120 min, almost the same as obtained at 210 min in the single system. Moreover, no Cr(III) was found to accumulate in solution in the binary system owing to the high adsorption capacity of TNS. Photocatalytic degradation of 4-CP was also enhanced in the binary system, with k_1 (0.0737 min^{-1}) about 2.6 times that for 4-CP photo-degradation in single system (0.0289 min^{-1}), and 98.1 % removal of 4-CP achieved by 60 min.

Therefore, synergetic promotion of the photocatalytic removal of Cr(VI) and 4-CP by TNS was found to occur when both coexisted in solution; this synergetic effect was closely related to the photocatalytic mechanism involved in the reactions.

[Fig . 6]

The first-order kinetic model simulation of photocatalysis in binary system is nonlinear and close to exponential (R^2 • 0.997, $\mathrm{Ln}(C_0/C_t) = t^n$ and n >1) (Fig. 6b), indicating that the photocatalytic reaction has accelerated with time for both Cr(VI) and 4-CP. Gradual photo-reduction of Cr(VI) resulted in formation of Cr(III), which was subsequently adsorbed by TNS. It should be noted that TNS with Cr(III) incorporated, and then substituted, acted like a autosynchronous doping process, thus enhancing the photocatalytic activity of TNS. Moreover, the amount of Cr(III) entering into TNS increased as time progressed, leading to gradually enhanced photocatalytic activity.

To further confirm this synergetic promotion effect, photocatalytic reduction of Cr(VI) in the presence of varying 4-CP concentrations was tested (Fig. S8), and Table S1 lists the corresponding first-order kinetic model parameters. The results indicate more 4-CP added leaded to higher Cr(VI) photocatalytic reduction rate. Even at 2.5 mg/L of 4-CP, the k_1 value was 0.0428 min^{-1}, about 2.6 times of that for Cr(VI) reduction without 4-CP. The k_1 value increased to 0.0735 min^{-1} when the coexisting 4-CP increased to 10 mg/L, indicating the progressive enhancement of the promotion effect by increasing the 4-CP concentration.

3.5 Synergetic promotion mechanism for photocatalysis of Cr(VI) and 4-CP

During photocatalysis, TNS can generate a conduction band (electron, e^-) and a valence band (hole, h^+) under UV irradiation (Eqn. 8). Then Cr(VI) is reduced to Cr(III) by the electrons (Eqn. 9). Meanwhile, the holes oxidize H_2O molecules into ROS (·OH, $\cdot O_2^-$, H_2O_2, etc.) (Eqns. 10í 15), and 4-CP is degraded through oxidation by these species [17, 18, 46, 50] (Eqn. 16).

$$\text{TNS (titanate/TiO}_2\text{)} + h\nu = \text{TNS*}\ (e^- \text{í}\ h^+) \quad (8)$$

$$HCrO_4^- + 7H^+ + 3e^- = Cr^{3+} + 4H_2O \quad (9)$$

$$2H_2O + 4h^+ = O_2 + 4H^+ \quad (10)$$

$$H_2O + h^+ : \quad \ddagger OH + H^+ \quad (11)$$

$$OH^- + h^+ \ : \ \ddagger OH \quad (12)$$

$$O_2 + e^- = \ddagger O_2^- \quad (13)$$

$$\ddagger O_2^- + e^- + 2H^+ = H_2O_2 \quad (14)$$

$$H_2O_2 + \ddagger O_2^- = HO\ddagger + OH^- + O_2 \quad (15)$$

$$\text{4-CP} + \ddagger OH\ (\text{or}\ \ddagger O_2^-, H_2O_2) : \quad \text{intermediates :SURGXFWV} \rightarrow CO_2 \quad (16)$$

Acidic conditions promote reduction of Cr(VI) according to Eqn. 9, whereas alkaline solution with abundant OH^- facilitates formation of ‡OH according to Eqns. 11 and 12. Hence, the removal efficiency of Cr(VI) was higher for photocatalysis at lower pH (Fig. 4), unlike less efficient at lower pH for 4-CP (Fig. 5).

Cr(III) has similar atomic size to Ti and so is widely used as a doping metal to modify TiO_2 and thereby enhance its photocatalytic performance [51-53]. EDS shows that Cr(III) successfully entered into TNS after reaction (Fig. S9). Cr 2p peak is also observed for TNS-Cr(III) in the XPS survey spectra (Fig. S10a). Moreover, high resolution of Cr 2p spectra indicates that all the incorporated Cr are in the form of

Cr(III) (E_b | 577 eV) (Fig. S10b) [29], suggesting complete photo-reduction of Cr(VI) by TNS. EDS and XPS analysis of TNS-Cr(III) confirmed autosynchronous doping of Cr(III) during the reaction. Fig. 7 presents the UV-vis DRS spectra of TNS before and after Cr(III) entered, and the energy band gaps (E_g) of the materials are calculated by Kubelka-Munk theory [54]. The light adsorption edge of the pure TNS was 399 nm with E_g = 3.1 eV, close to that of TiO_2 type P25 and titanate nanotubes [31, 55]. After Cr(III) doping of TNS (TNS-Cr(III)), the adsorption edge shifted to the visible light range of 448 nm, and the E_g value decreased to 2.8 eV. In addition, band gap of titanate in the composite material is more likely to be narrowed due to efficient capture of Cr(III). Here, the narrowed energy band gap implies that a much wider light range was utilized in the photocatalytic reaction.

[Fig. 7]

After incorporation into TNS, the Cr^{3+} trapped holes photo-generated by titanate or in Cr^{4+} by TiO_2 that further reacted with OH^- to produce hydroxyl radicals (Eqns. 17 and 18) [53]. Hence, recombination of hole-electron pairs became inhibited due to the presence of the hole media, Cr^{3+}. Besides, Cr(III) can also act as a donor level to produce electrons under UV light, followed by production of ‡O_2^- (Eqns. 19 and 20) [18, 53], which is a strong ROS that can further degrade 4-CP.

$Cr^{3+} + h^+ :\quad Cr^{4+}$ (17)

$Cr^{4+} + OH^- :\quad Cr^{3+} +$ ‡+ (18)

$Cr^{3+} + K :\quad Cr^{4+} + e^-$ (19)

$e^- + O_2 :\quad$ ‡ $_2^-$ (20)

Fig. S11 further confirms the increased ‡OH production by TNS after Cr(III) doping, and the higher Cr doping dosage resulting in larger QXPEHUVRI‡OH radicals. In short, Cr autosynchronous doping helps to facilitate the photocatalytic degradation of 4-CP due to the increased abundance of ROS produced. Fig. S12 shows the photocatalytic degradation pathway of 4-CP in the binary system based on GC spectra (Fig. S13) and MS confirmation (Table S2), which is discussed in detail in **Supplementary data**. It is also found that the proposed 4-CP degradation pathway is similar to that for photocatalysis by TiO_2 or other oxidation processes reported previously [19, 56-58].

Fig. 8 depicts the synergetic promotion effect and autosynchronous doping process for simultaneous removal of Cr(VI) and 4-CP. TNS is a composite material with combined crystalline phases of anatase and titanate. Under light irradiation, TNS (mainly the anatase phase) generates a conduction band (e^-) and a valance band (h^+). Cr(VI) reduces to Cr(III) after acceptance of e^- (Reaction 1), while oxidative degradation of 4-CP by ROS also occurs (Reaction 2) with the help of h^+. Continuous consumption of electrons and holes for photocatalytic reduction and oxidation in the same system leads to efficient separation of the h^+í e^- pairs and thus a synergetic promotion effect occurs with coexistent Cr(VI) and 4-CP. Moreover, the photo-reduced Cr(III) can be immediately adsorbed and incorporated into titanate (Reaction 3), which is a autosynchronous promoted process that can enhance the photocatalytic activity of TNS through narrowing the band of the energy gap (from 3.1 to 2.8 eV). An important finding is that both photo-reduction of Cr(VI) and

photo-degradation of 4-CP are greatly promoted in binary systems, due to the dual mechanisms of synergic promotion and autosynchronous doping.

[Fig. 8]

3.6 Reuse of TNS

After photocatalysis, we carried out a two-step procedure to regenerate TNS, following our previous studies [18, 59]. Adsorbed Cr(III) was desorbed from TNS through 0.5 M HNO_3 treatment, while adsorption sites (í ONa groups) were restored through further 0.5 M NaOH treatment. The regenerated material was reused for photocatalytic removal of coexisting Cr(VI) and 4-CP over 5 cycles in total, and results are shown in Fig. 9. TNS demonstrated good reusability potential, with the removal efficiency of total Cr and Cr(VI) could still reaching 97.8% by 210 min photocatalysis after the beginning of each reuse cycle, even at the 5^{th} cycle, and no Cr(III) was detected in the solution. Similarly, the removal efficiency of 4-CP was as high as 99.3% in the 5^{th} cycle. It should also be noted that titanate nanomaterials can be easily separated from solution due to their heterogeneous structure/composition compared to nano-TiO_2 [60]. The simple regeneration procedure and good reusability of TNS make it a promising material for environmental remediation, especially in the treatment of complex contaminants involving the co-existence of heavy metals and organic pollutants.

[Fig. 9]

4. Conclusions

An anatase/titanate nanosheet composite material was synthesized through a

facile one-step hydrothermal treatment and used to simultaneously remove Cr(VI) and 4-CP from waters, and the main conclusions are summarized as:

(1) The prepared TNS is a composite material involving anatase attached onto titanate, of which titanate is the main adsorption site while anatase acts as primary the photocatalytic center.

(2) TNS exhibited high capacity for the adsorption of cationic Cr(III), but was ineffective at capturing anionic Cr(VI) and molecular 4-CP. While upon photocatalysis, Cr(VI) was reduced by 97.2% at pH 7, and the formed Cr(III) was simultaneously adsorbed onto TNS. Moreover, >99% of 4-CP was photo-degraded by TNS at pH 5í 9.

(3) In a binary photocatalysis system with co-existent of Cr(III) and 4-CP, the removal efficiencies of both contaminants were enhanced compared to those achieved in single systems under the same conditions, with the apparent rate constant (k_1) for photocatalysis removal of Cr(VI) and 4-CP increasing by factors of about 3.1 and 2.6, respectively.

(4) Mechanisms for enhanced removal efficiency with co-existent Cr(III) and 4-CP are attributed to synergetic photocatalysis and autosynchronous doping. The combination of photo-reduction of Cr(VI) by electrons and photo-degradation of 4-CP by holes causes efficient separation of electron-hole pairs. Moreover, adsorption of Cr(III) by TNS leads to narrowed energy band gap and enhanced photocatalytic activity of the materials.

(5) TNS could be efficiently reused for photocatalytic removal of Cr(VI) and

4-CP, as 97.8% and 99.3% removal efficiencies of the two pollutants were achieved even after 5 cycles, respectively.

Acknowledgement

Financial support from the National Natural Science Foundation of China (No. 51508006) and the Natural Science Foundation of the Colleges and Universities in Jiangsu Province (15KJB610011) are much appreciated.

Appendix A. Supplementary data

Supplementary data related associated with this article can be found in the online version.

References

[1] V.M. Correia, T. Stephenson, S.J. Judd, Characterization of textile wastewaters - a review, Environ. Technol. 15 (1994) 917-929.

[2] X. He, X. Nie, Z. Wang, Z. Cheng, K. Li, G. Li, M.H. Wong, X. Liang, M.T.K. Tsui, Assessment of typical pollutants in waterborne by combining active biomonitoring and integrated biomarkers response, Chemosphere 84 (2011) 1422-1431.

[3] S.J. Edwards, B.V. Kjellerup, Applications of biofilms in bioremediation and biotransformation of persistent organic pollutants, pharmaceuticals/personal care products, and heavy metals, Appl. Microbiol. Biot. 97 (2013) 9909-9921.

[4] M. Tripathi, S.K. Garg, Dechlorination of chloroorganics, decolorization, and simultaneous bioremediation of Cr^{6+} from real tannery effluent employing indigenous *Bacillus cereus* isolate, Environ. Sci. Pollut. R 21 (2014) 5227-5241.

[5] M. Tripathi, S. Vikram, R.K. Jain, S.K. Garg, Isolation and growth characteristics of chromium(VI) and pentachlorophenol tolerant bacterial isolate from treated tannery effluent

for its possible use in simultaneous bioremediation, Indian J. Microbiol. 51 (2011) 61-69.

[6] M. Costa, Toxicity and carcinogenicity of Cr(VI) in animal models and humans, Crit. Rev. Toxicol. 27 (1997) 431-442.

[7] A. Sorokin, J.L. Seris, B. Meunier, Efficient oxidative dechlorination and aromatic ring-cleavage of chlorinated phenols catalyzed by iron sulfophthalocyanine, Science 268 (1995) 1163-1166.

[8] M.F.F. Sze, G. McKay, Enhanced mitigation of para-chlorophenol using stratified activated carbon adsorption columns, Water Res. 46 (2012) 700-710.

[9] Z. Aksu, J. Yener, A comparative adsorption/biosorption study of mono-chlorinated phenols onto various sorbents, Waste Manage. 21 (2001) 695-702.

[10] M. Ahmaruzzaman, Adsorption of phenolic compounds on low-cost adsorbents: A review, Sci Adv. Colloid Interface Sci. 143 (2008) 48-67.

[11] C. Quintelas, E. Sousa, F. Silva, S. Neto, T. Tavares, Competitive biosorption of ortho-cresol, phenol, chlorophenol and chromium(VI) from aqueous solution by a bacterial biofilm supported on granular activated carbon, Process Biochem. 41 (2006) 2087-2091.

[12] J.P. Scott, D.F. Ollis, Integration of chemical and biological oxidation processes for water treatment: Review and recommendations, Environ. Prog. 14 (1995) 88-103.

[13] L. Huang, X. Chai, X. Quan, B.E. Logan, G. Chen, Reductive dechlorination and mineralization of pentachlorophenol in biocathode microbial fuel cells, Bioresource Technol. 111 (2012) 167-174.

[14] X. Yin, W. Liu, J. Ni, Removal of coexisting Cr(VI) and 4-chlorophenol through reduction and Fenton reaction in a single system, Chem. Eng. J. 248 (2014) 89-97.

[15] C.E. Barrera-Diaz, V. Lugo-Lugo, B. Bilyeu, A review of chemical, electrochemical and biological methods for aqueous Cr(VI) reduction, J. Hazard. Mater. 223 (2012) 1-12.

[16] D. He, X. Guan, J. Ma, X. Yang, C. Cui, Influence of humic acids of different origins on oxidation of phenol and chlorophenols by permanganate, J. Hazard. Mater. 182 (2010) 681-688.

[17] R. Qiu, D. Zhang, Z. Diao, X. Huang, C. He, J.-L. Morel, Y. Xiong, Visible light induced photocatalytic reduction of Cr(VI) over polymer-sensitized TiO_2 and its synergism with phenol oxidation, Water Res. 46 (2012) 2299-2306.

[18] W. Liu, J. Ni, X. Yin, Synergy of photocatalysis and adsorption for simultaneous removal of Cr(VI) and Cr(III) with TiO_2 and titanate nanotubes, Water Res. 53 (2014) 12-25.

[19] Y. Cheng, H. Sun, W. Jin, N. Xu, Photocatalytic degradation of 4-chlorophenol with combustion synthesized TiO_2 under visible light irradiation, Chem. Eng. J. 128 (2007) 127-133.

[20] R. Daghrir, P. Drogui, D. Robert, Modified TiO_2 For Environmental Photocatalytic Applications: A Review, Ind. Eng. Chem. Res. 52 (2013) 3581-3599.

[21] C. Lettmann, K. Hildenbrand, H. Kisch, W. Macyk, W.F. Maier, Visible light photodegradation of 4-chlorophenol with a coke-containing titanium dioxide photocatalyst, Appl. Catal. B-Environ. 32 (2001) 215-227.

[22] W. Liu, T. Wang, A.G.L. Borthwick, Y. Wang, X. Yin, X. Li, J. Ni, Adsorption of Pb^{2+}, Cd^{2+}, Cu^{2+} and Cr^{3+} onto titanate nanotubes: Competition and effect of inorganic ions, Sci. Total. Environ. 456 (2013) 171-180.

[23] T. Kasuga, M. Hiramatsu, A. Hoson, T. Sekino, K. Niihara, Titania nanotubes prepared by chemical processing, Adv. Mater. 11 (1999) 1307-1311.

[24] D.V. Bavykin, J.M. Friedrich, F.C. Walsh, Protonated titanates and TiO_2 nanostructured materials: Synthesis, properties, and applications, Adv. Mater. 18 (2006) 2807-2824.

[25] L. Xiong, C. Chen, Q. Chen, J. Ni, Adsorption of Pb(II) and Cd(II) from aqueous solutions using titanate nanotubes prepared via hydrothermal method, J. Hazard. Mater. 189 (2011) 741-748.

[26] X.M. Sun, Y.D. Li, Synthesis and characterization of ion-exchangeable titanate nanotubes, Chem.-Eur. J. 9 (2003) 2229-2238.

[27] W. Liu, H. Chen, A.G.L. Borthwick, Y. Han, J. Ni, Mutual promotion mechanism for adsorption of coexisting Cr(III) and Cr(VI) onto titanate nanotubes, Chem. Eng. J. 232 (2013) 228-236.

[28] Y. Wang, W. Liu, T. Wang, J. Ni, Arsenate adsorption onto Fe-TNTs prepared by a novel water-ethanol hydrothermal method: Mechanism and synergistic effect, J. Colloid Interface Sci. 440 (2015) 253-262.

[29] L. Wang, W. Liu, T. Wang, J. Ni, Highly efficient adsorption of Cr(VI) from aqueous solutions by amino-functionalized titanate nanotubes, Chem. Eng. J. 225 (2013) 153-163.

[30] J.G. Yu, H.G. Yu, B. Cheng, C. Trapalis, Effects of calcination temperature on the microstructures and photocatalytic activity of titanate nanotubes, J. Mol. Catal. A-Chem. 249 (2006) 135-142.

[31] W. Liu, X. Zhao, A.G.L. Borthwick, Y. Wang, J. Ni, Dual-enhanced photocatalytic activity of Fe-deposited titanate nanotubes used for simultaneous removal of As(III) and As(V), ACS Appl. Mater. Interfaces 7 (2015) 19726-19735.

>@;=KDR=8L7:DQJ6(2¶HLOO\/LX'=KDR$QHZ WSH RI FREDOW -deposited titanate nanotubes for enhanced photocatalytic degradation of phenanthrene, Appl. Catal. B-Environ. 187 (2016) 134-143.

[33] J.C. Crittenden, J.B. Liu, D.W. Hand, D.L. Perram, Photocatalytic oxidation of chlorinated hydrocarbons in water, Water Res. 31 (1997) 429-438.

[34] X. Li, W. Liu, J. Ni, Short-cut synthesis of tri-titanate nanotubes using nano-anatase: Mechanism and application as an excellent adsorbent, Micropor. Mesopor. Mater. 213 (2015) 40-47.

[35] L. Rizzo, S. Meric, D. Kassinos, M. Guida, F. Russo, V. Belgiorno, Degradation of diclofenac by TiO_2 photocatalysis: UV absorbance kinetics and process evaluation through a set of toxicity bioassays, Water Res. 43 (2009) 979-988.

[36] C.N. Satterfield, Mass Transfer in Heterogeneous Catalysis, MIT Press, Cambridge, MA, UK 1970.

[37] J.P.S. Valente, P.M. Padilha, A.O. Florentino, Studies on the adsorption and kinetics of photodegradation of a model compound for heterogeneous photocatalysis onto TiO_2, Chemosphere 64 (2006) 1128-1133.

[38] Q. Chen, W.Z. Zhou, G.H. Du, L.M. Peng, Trititanate nanotubes made via a single alkali treatment, Adv. Mater. 14 (2002) 1208-1211.

[39] J. Zhang, Y. Zhang, Y. Lei, C. Pan, Photocatalytic and degradation mechanisms of anatase TiO_2: a HRTEM study, Catal. Sci. Technol. 1 (2011) 273-278.

[40] H.G. Yang, C.H. Sun, S.Z. Qiao, J. Zou, G. Liu, S.C. Smith, H.M. Cheng, G.Q. Lu, Anatase TiO_2 single crystals with a large percentage of reactive facets, Nature 453 (2008) 638-641.

[41] L. Gu, J. Wang, H. Cheng, Y. Du, X. Han, Synthesis of nano-sized anatase TiO_2 with reactive {001} facets using lamellar protonated titanate as precursor, Chem. Commun. 48 (2012)

6978-6980.

[42] R.Z. Ma, K. Fukuda, T. Sasaki, M. Osada, Y. Bando, Structural features of titanate nanotubes/nanobelts revealed by Raman, X-ray absorption fine structure and electron diffraction characterizations, J. Phys. Chem. B 109 (2005) 6210-6214.

[43] S. Brunauer, L.S. Deming, W.E. Deming, E. Teller, On a theory of the van der Waals adsorption of gases, J. Am. Chem. Soc. 62 (1940) 1723-1732.

[44] P. Wen, H. Itoh, W. Tang, Q. Feng, Single nanocrystals of anatase-type TiO_2 prepared from layered titanate nanosheets: Formation mechanism and characterization of surface properties, Langmuir 23 (2007) 11782-11790.

[45] T. Wang, W. Liu, L. Xiong, N. Xu, J. Ni, Influence of pH, ionic strength and humic acid on competitive adsorption of Pb(II), Cd(II) and Cr(III) onto titanate nanotubes, Chem. Eng. J. 215 (2013) 366-374.

[46] S. Kim, W. Choi, Visible-light-induced photocatalytic degradation of 4-chlorophenol and phenolic compounds in aqueous suspension of pure titania: Demonstrating the existence of a surface-complex-mediated path, J. Phys. Chem. B 109 (2005) 5143-5149.

[47] R. Vinu, G. Madras, Kinetics of simultaneous photocatalytic degradation of phenolic compounds and reduction of metal ions with nano-TiO_2, Environ. Sci. Technol. 42 (2008) 913-919.

[48] S.L. Wang, C.C. Chen, Y.M. Tzou, C.L. Hsu, J.H. Chen, C.F. Lin, A mechanism study of light-induced Cr(VI) reduction in an acidic solution, J. Hazard. Mater. 164 (2009) 223-228.

[49] R.A. Doong, C.H. Chen, R.A. Maithreepala, S.M. Chang, The influence of pH and cadmium sulfide on the photocatalytic degradation of 2-chlorophenol in titanium dioxide suspensions, Water Res. 35 (2001) 2873-2880.

[50] Y. Hou, X. Li, X. Zou, X. Quan, G. Chen, Photoeletrocatalytic activity of a Cu_2O-loaded self-organized highly oriented TiO_2 nanotube array electrode for 4-chlorophenol degradation, Environ. Sci. Technol. 43 (2009) 858-863.

[51] S.M. Zhang, Y.Y. Chen, Y. Yu, H.H. Wu, S.R. Wang, B.L. Zhu, W.P. Huang, S.H. Wu, Synthesis, characterization of Cr-doped TiO_2 nanotubes with high photocatalytic activity, J. Nanopart. Res. 10 (2008) 871-875.

[52] X. Fan, X. Chen, S. Zhu, Z. Li, T. Yu, J. Ye, Z. Zou, The structural, physical and

photocatalytic properties of the mesoporous Cr-doped TiO_2, J. Mol. Catal. A-Chem. 284 (2008) 155-160.

[53] J.F. Zhu, Z.G. Deng, F. Chen, J.L. Zhang, H.J. Chen, M. Anpo, J.Z. Huang, L.Z. Zhang, Hydrothermal doping method for preparation of Cr^{3+}-TiO_2 photocatalysts with concentration gradient distribution of Cr^{3+}, Appl. Catal. B-Environ. 62 (2006) 329-335.

[54] N. Serpone, D. Lawless, R. Khairutdinov, Size effects on the photophysical properties of colloidal anatase TiO_2 particles - size quantization or direct transitions in this indirect semiconductor, J. Phys. Chem. 99 (1995) 16646-16654.

[55] R. Lopez, R. Gomez, Band-gap energy estimation from diffuse reflectance measurements on sol-gel and commercial TiO_2: a comparative study, J. Sol-gel. Sci. Techn. 61 (2012) 1-7.

[56] Z.H. Ai, P. Yang, X.H. Lu, Degradation of 4-chlorophenol by a microwave assisted photocatalysis method, J. Hazard. Mater. 124 (2005) 147-152.

[57] S.K. Johnson, L.L. Houk, J.R. Feng, R.S. Houk, D.C. Johnson, Electrochemical incineration of 4-chlorophenol and the identification of products and intermediates by mass spectrometry, Environ. Sci. Technol. 33 (1999) 2638-2644.

[58] J. Zhao, Y. Zhang, X. Quan, S. Chen, Enhanced oxidation of 4-chlorophenol using sulfate radicals generated from zero-valent iron and peroxydisulfate at ambient temperature, Sep. Purif. Technol. 71 (2010) 302-307.

[59] T. Wang, W. Liu, N. Xu, J. Ni, Adsorption and desorption of Cd(II) onto titanate nanotubes and efficient regeneration of tubular structures, J. Hazard. Mater. 250 (2013) 379-386.

[60] W. Liu, W. Sun, A.G.L. Borthwick, J. Ni, Comparison on aggregation and sedimentation of titanium dioxide, titanate nanotubes and titanate nanotubes-TiO_2: Influence of pH, ionic strength and natural organic matter, Colloids Surf. A 434 (2013) 319-328.

Figures

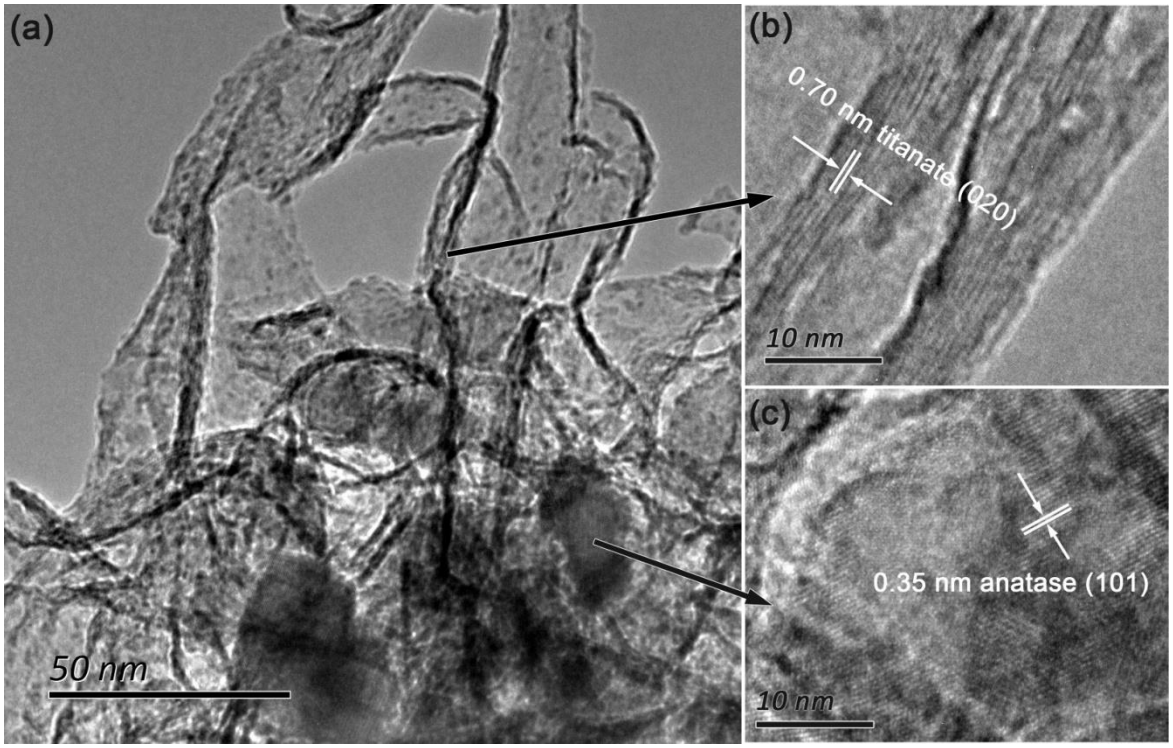

Fig. 1. TEM images of (a) TNS and HRTEM of (b) titanate and (c) anatase in TNS.

Fig. 2. XRD patterns of nano-TiO_2 and TNS.

Fig. 3. Adsorption capacity at equilibrium of Cr(VI), Cr(III) and 4-CP by TNS as pH varies from 2 to 9. (Experimental conditions: initial Cr and 4-chorophenol = 5 mg/L, TNS dosage = 0.5 g/L, temperature = 25±2 qC).

Fig. 4. Variation of Cr(total), Cr(VI) and Cr(III) with irradiation time during the photocatalysis process at pH = 5, 7 and 9. (Experimental conditions: initial Cr(VI) = 5 mg/L, TNS dosage = 0.5 g/L, temperature = 25±2 qC).

Fig. 5. Variation of 4-CP with irradiation time during the photocatalysis process at pH = 5, 7 and 9. (Experimental conditions: initial 4-CP = 5 mg/L, TNS dosage = 0.5 g/L, temperature = 25±2 qC).

Fig. 6. Variation of Cr(total), Cr(VI), Cr(III) and 4-CP in binary systems with irradiation time: (a) photocatalysis of by TNS; and (b) first-order kinetic model fits to time-dependent photocatalysis of Cr(VI) and 4-CP. (Experimental conditions: initial Cr(VI) and 4-CP = 5 mg/L, TNS dosage = 0.5 g/L, solution pH = 7, temperature =25±2 qC).

Fig. 7. Absorbance UV-vis diffuse reflectance spectra (DRS) of TNS before and after Cr(III) is introduced.

Fig. 8. Schematic diagram for synergetic promotion and autosynchronous doping in photocatalysis.

Fig. 9. Reuse of TNS for photocatalytic removal of Cr(VI) and 4-CP in the binary system over 5 cycles. (Experimental conditions: initial Cr(VI) and 4-CP = 5 mg/L, TNS dosage = 0.5 g/L, solution pH =7, temperature =25±2 qC).

Table legend

Table 1. Parameters of first-order kinetic model for photocatalytic removal of Cr(VI) and 4-CP for various pH values.

System	pH	First -order model	
		k_1 (min^{-1})	R^2
Single Cr(VI)	5	0.0240	0.9944
	7	0.0164	0.9903
	9	0.0087	0.9941
Single 4-CP	5	0.0221	0.9917
	7	0.0289	0.9970
	9	0.0399	0.9975
Binary Cr(VI)	7	0.0502	0.9756
Binary 4-CP	7	0.0737	0.9854